Detailed Design and RF Analysis of a Scatterometer for Material Characterization in the 50-750 GHz Range

C. Cappellin[1], P. H. Nielsen[1], R. Appleby[2], R. Wylde[3], E. Saenz[4]
[1] TICRA, Copenhagen, Denmark, cc@ticra.com, phn@ticra.com
[2] Roger Appleby MMW Consulting, Malvern link, Worcs, UK, applebyroger@yahoo.co.uk
[3] Thomas Keating Ltd., Billingshurst, West Sussex, UK
[4] ESA/ESTEC, Noordwijk, The Netherlands

***Abstract*—This paper describes the detailed electromagnetic modelling and design of a scatterometer to be used at the European Space Agency, for characterization in transmission and reflection of smooth as well as rough materials in the 50-750 GHz region. The scatterometer is analysed with the software GRASP. The initial design based on quasi-optics showed poor performances and was thus modified significantly, obtaining improvements in beam quality, beam displacement and cross-polar performance.**

***Index Terms*—materials, measurement.**

I. Introduction

Dielectrics, frequency selective surfaces (FSS), sandwich structures, composite resins, ceramics and metal plates are used in antenna applications ranging from low frequencies up to sub-mm waves. An accurate characterization of these materials is of vital importance in predicting the performances of future missions in Telecom, Earth Observations and Science.

Materials are typically characterized in terms of reflection, transmission and absorption. To measure these parameters, well-known procedures and instruments exist for homogeneous materials with smooth surfaces [1]. For inhomogeneous or rough materials, however, the accuracy of the measurements is strongly affected by the field which is scattered away from the material. This scattering is a function of the dielectric constant of the material, the wavelength and the angle of incidence and occurs in both transmission and reflection. To fully characterize an inhomogeneous and rough material, it is therefore essential to measure its scattered radiation. The measured scattered radiation is then used to correct reflectivity and transmission measurements to avoid the scattering being considered as absorption. The angular distribution of the scattering for relatively smooth samples can also be used to estimate the physical properties of the surface [2]. Once accurately measured, the reflection and transmission properties of the materials shall be included in the detailed RF simulations of the antenna system in its environment, to obtain the final performance.

Measuring scattering radiation requires a system in which the properties of the materials can be investigated over a wide frequency band, a wide range of incidence and scattering angles. This calls for a free space system in which these angles can be adjusted.

The objectives of the ESA contract 4000116424/16 awarded to Roger Appleby MMW Consulting, Thomas Keating, Pixel Analytics and TICRA, was to design, manufacture and test a scatterometer according to the principles described above for accurate scattering measurements in the 50-750 GHz region of the spectrum. The initial design of the instrument was based on a periscope, which rotates around the sample enabling the network analyser extenders and associated cables to remain static, as previously reported by Lo et al. [3].

This paper focuses on the RF modelling of the initial scatterometer in the GRASP software, in Section II, and on the modifications introduced to the initial design to improve the instrument performances in Section III. In Section IV the improved design is analysed in reflection and transmission for rough samples and in Section V the detailed RF analysis of the periscope walls are provided, arriving at the final design, which is currently being tested. A detailed description of the instrument, its calibration as well as the algorithms used to extract the material properties are given in [4].

II. Initial Design and Grasp Analysis

The initial design of the scatterometer was based on ray tracing techniques and free space standard ellipsoidal mirrors with a focal length of 250 mm [5]. The operational frequency range is divided into 7 frequency sub-bands, and for each band a different corrugated horn and extended Vector Network Analyser (VNA) head is required. Two optical benches, one positioned above the other and separated by a distance of two times the focal length of the ellipsoids, are used. The two base plates are linked by a periscope, which rotates around a vertical axis passing through the sample, allowing the collection of the scattered radiation. The angle of rotation of the periscope is computed relative to the axis that connects the center of the sample with the center of the mirror illuminating the sample. The range of the rotation angle of the periscope for reflection in the sample is [36°:90°]. The sample can also be rotated around its vertical axis. A sample rotation of 0° means that the normal to the sample is aligned with the axis that connects the center of the sample with the center of the mirror illuminating the sample. The VNA heads remain stationary.

As shown in Fig. 1, the beam is launched at the back right corner of the lower plate from the VNA head 1 via a corrugated horn, and is focused by a mirror to a beam waist at the sample. Scattered radiation from the sample falls on the lower mirror of the periscope and is then relayed on to an upper mirror. From here there are two possible paths, one for transmission and one for reflection. This is necessary to maintain an acute angle at the redirection mirror.

The scatterometer was modelled in the GRASP software in order to accurately compute the beam's quality, coupling loss and cross-polar performance over the full frequency band and a wide range of incidence and scattering angles. We considered initially as a sample a smooth flat mirror in specular reflection, i.e. at 45° rotation with 90° rotation of the periscope, which can be used in the calibration of the scatterometer, as depicted in Fig. 1.

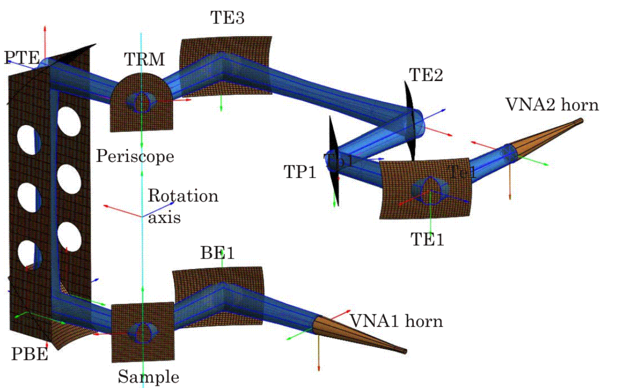

Fig. 1. GRASP model of the initial scatterometer, with a Gaussian beam launched from the VNA1 horn, and reflection on the smooth sample for a 90° rotation of the periscope, and 45° rotation of the sample. The size of the sample is 125 mm by 125 mm.

The RF performance of the scatterometer is calculated in GRASP using Physical Optics (PO), on all the mirrors and the sample. For samples with roughness correlation lengths smaller than a wavelength Method of Moment (MoM) on the sample is required. These methods give the exact RF scattering from the mirrors and sample, including the higher order Gaussian modes generated by the offset ellipsoids. The power received by the VNA2 horn is extracted using the Coupling add-on to GRASP. The PO analysis of the scatterometer also provides a value of the spill-over losses through the system. Identical corrugated horns described by spherical wave expansion (SWE) coefficients provided by Thomas Keating Limited are used in VNA1 and VNA2 and imported into GRASP.

The incident field on the sample surface calculated by GRASP at 94 GHz showed that, due to the offset geometry of the first ellipsoidal mirror BE1, the cross-polarization level of the incident field on the sample surface increases from the 40 dB below the peak at VNA1, to 25 dB below the peak. The field on the aperture of the receiving horn, VNA2, showed that the cross-polarization is increased further through the offset mirrors in the periscope and all the other mirrors on the top base plate, resulting in a final cross-polar level of 16 dB below the peak. Furthermore, the co-polar beam waist is deformed to 9 mm × 9.5 mm and the waist is displaced 2.2 mm in the horizontal direction. Similar conclusions were drawn at higher frequencies.

III. GRASP Analysis of the Modified Design

The GRASP analysis of the initial design shown in Section II revealed that the system suffered from beam displacement, poor cross-polar performance and poor beam quality. This implied that for some samples the scattered radiation would have fallen below the signal to noise ratio of the VNA. Several modifications to the initial design were then studied in GRASP, and, on the basis of the results, the design was modified significantly. The final design is shown in Fig. 2 for reflection and in Fig. 3 for transmission.

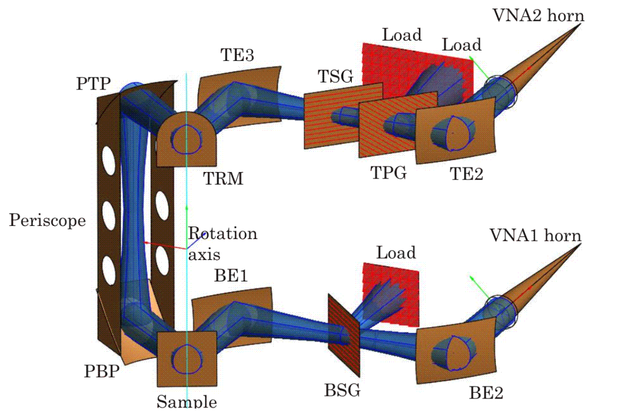

Fig. 2. GRASP model of the final scatterometer in reflection for 50° rotation of the periscope, and 25° rotation of the sample.

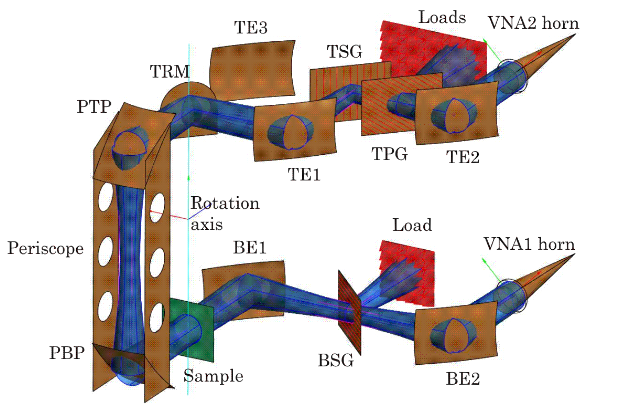

Fig. 3. GRASP model of the final scatterometer in transmission for 180° rotation of the periscope and 0° rotation of the sample.

Relative to the initial design of Fig. 1, the two ellipsoids in the periscope were replaced by two paraboloids, which provide a compensated design which thus does not introduce cross-polarization. Secondly, the number of ellipsoids on the top and bottom base plates was changed as well as their orientation, in order to use a compensated design where the ellipsoids are in a Z configuration. Introducing an additional ellipsoid in the bottom base plate also implies that the sample lies at a relayed focus, where there is a much smaller beam waist. This has the clear advantage of increasing the solid angle at the sample, especially at the high frequencies, giving a proportional increase in signal level. Finally, the two single linear-polarized horns are rotated 45 degrees in order to transmit and receive both horizontal and vertical polarization, when rotating the polarisation with grids BSG and TSG. The extra polarisation grid TPG is added in order to reject the cross-polar reflection in the receiving horn, VNA2. It is noted that the polarization grid BSG re-introduces the cross-polar component that the compensated design of BE1 and BE2 had removed. For transmission operation an extra mirror, TE1, is added to the scatterometer, and the polarisation grid TSG is rotated 90° in order to reflect the beam.

For the same sample made by a flat mirror in specular reflection, as in Section II and shown in Fig. 2, it is now seen that the cross-polarisation level of the incident field on the sample is still 25 dB below peak, because of the presence of BSG, and the co-polar beam waist size has decreased significantly relative to the initial design, as expected. On the receiving horn aperture plane, see Fig. 4, no displacement of the beam peak is generated and the beam is circular with a waist of 9.1 mm as shown by the -8.7 dB contour line. The cross-polar level of the incident field is unchanged through the system and remains at 25 dB below the peak.

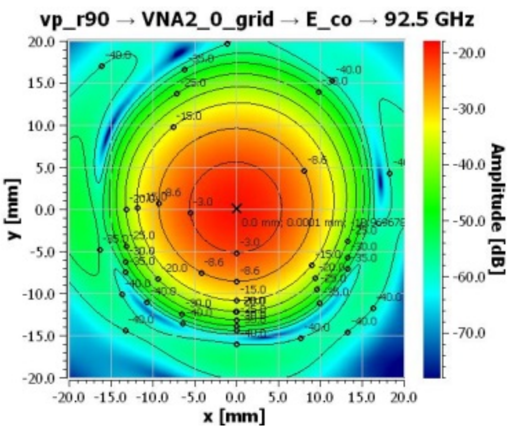

Fig. 4. Incident co-polar field on the aperture of the receiving horn at 92.5 GHz for the scatterometer of Fig. 2 and smooth flat sample at 45° with 90° periscope rotation.

IV. GRASP Analysis of Rough Samples

The RF performances of the scatterometer of Section III are now analysed at 62.5 GHz for a rough sample, fixed at an angle of 18° and for both reflection and transmission. The Method of Moments (MoM) add-on to GRASP is used to calculate the currents on the sample.

A. *Conducting rough sample for reflection case*

The conducting rough sample geometry is made by a random surface with grid spacing of 5 mm and surface peak to peak of ±0.5 mm. This gives a maximum correlation length of 10 mm and an rms value of 0.23 mm.

For the periscope in 36° rotation angle, the specular reflection from the sample illuminates the bottom mirror of the periscope and is then reflected and focused through the top mirrors to the VNA2 horn. The incident field on the aperture plane of the receiving horn is shown in Fig. 5, where it is seen that the beam waist still exists but is deformed and displaced by 8 mm. When the periscope is rotated 90°, the bottom mirror of the periscope is illuminated by the scattered field from the rough sample only. Therefore, the incident field on this periscope mirror is without any waist and much lower than the specular beam. The mirror collects the power of this scattered field and reflects it up to the top mirror of the periscope and focusses it through the top mirrors. The collected scattered field on the receiving horn aperture is shown in Fig. 6, having a beam peak of 26 dB below the specular beam.

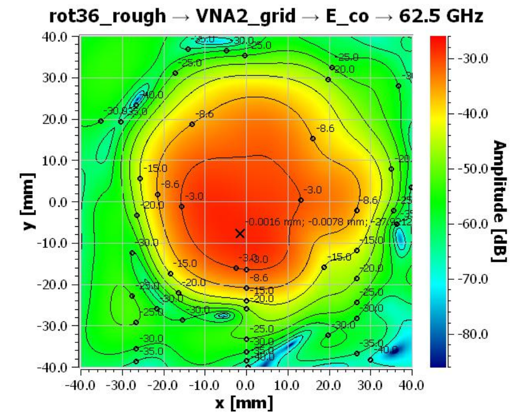

Fig. 5. Incident co-polar field on the aperture of the receiving horn for 36° periscope rotation and rough conducting sample at 18°.

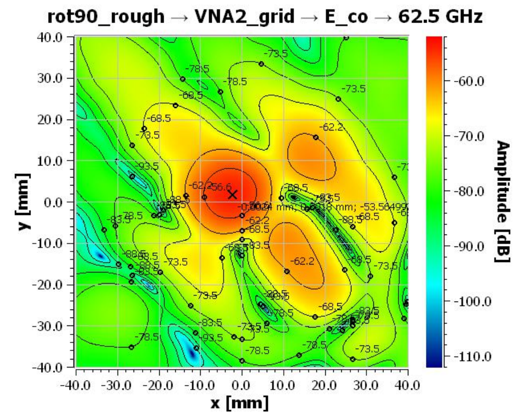

Fig. 6. Incident co-polar field on the aperture of the receiving horn for 90° periscope rotation and rough conducting sample at 18°.

The coupling to the VNA2 horn is then compared with the far-field of the sample found by illuminating it with a Gaussian beam with the same waist as the one created by the scatterometer. This comparison for varying periscope rotation angles with 6° interval is seen in Fig. 7, for the smooth and rough sample. It is observed that, besides a scaling factor, the coupling values with the rough sample well represent the far-field of it. The coupling values with the smooth sample draw a curve which is a bit broader than the corresponding far field. This is due to the finite aperture size of the periscope bottom mirror, which collects only a part of the scattered near field power.

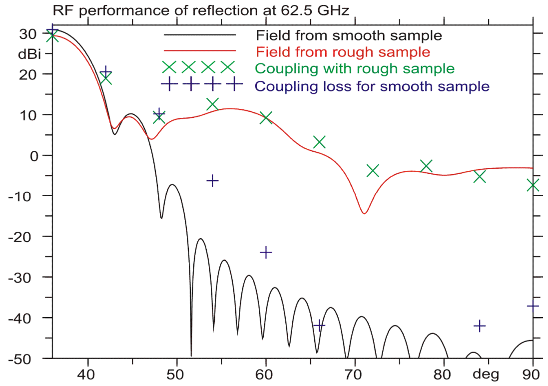

Fig. 7. Coupling values from conducting smooth and rough sample for varying periscope rotations, compared with simple scattered far-field of the sample.

B. Dielectric rough sample for transmission case

The dielectric rough sample used in the transmission case is shown in Fig. 8. The surface grid spacing of the random distortion is still 5 mm, but the surface peak to peak is increased to ±3 mm. This gives a maximum correlation length of 10 mm and an rms value of 1.4 mm. The dielectric constant of the sample is chosen equal to $\varepsilon_r = 2.025$ and the tangent loss is $\delta = 0.002$. The thickness of the sample is selected for maximum transmission to $3\lambda_\varepsilon/2$ equal to 5 mm at 62.5 GHz, where λ_ε is the wavelength in the dielectric.

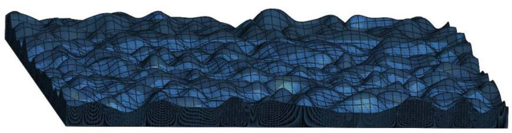

Fig. 8. Rough dielectric sample for the transmission case.

When the periscope is rotated 180° and for a sample orientation of 0°, as seen in Fig. 3, the beam illuminates the sample in normal incidence and the transmitted beam illuminates the bottom mirror of the periscope. The generated beam waist on the bottom periscope mirror will be deformed for rough sample, but it will still be in the centre of the mirror. After focusing through the top mirrors, the incident field on the VNA2 horn aperture plane is generated, see Fig. 9. It is seen that the beam waist still exists but is deformed and displaced by 9 mm.

When the periscope is rotated 216° and away from the specular transmission, the bottom mirror of the periscope is illuminated by the scattered field through the rough surface. The incident field on the periscope bottom mirror does not have a waist and is much lower than at 180° rotation. The bottom mirror of the periscope collects the power of the scattered field and, through the top mirrors, sends it to the VNA2 horn. The field incident on VNA2 is seen in Fig. 10. It is seen that the scattered transmitted field has nearly been focused and collected by the scatterometer with a beam peak of 17 dB below the transmission beam of Fig. 9.

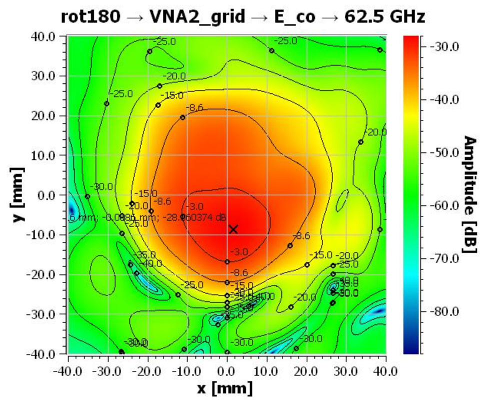

Fig. 9. Incident co-polar field on VNA2 aperture plane for 180° rotation and rough dielectric sample.

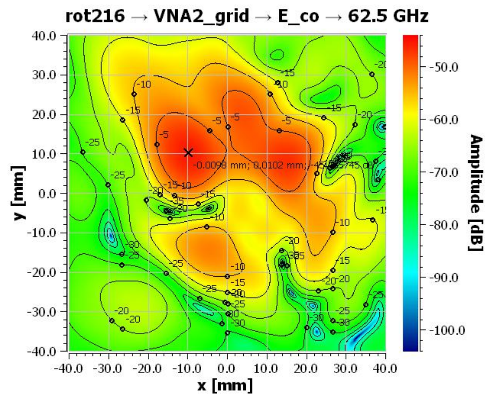

Fig. 10. Incident co-polar field on VNA2 aperture plane for 216° rotation and rough dielectric sample.

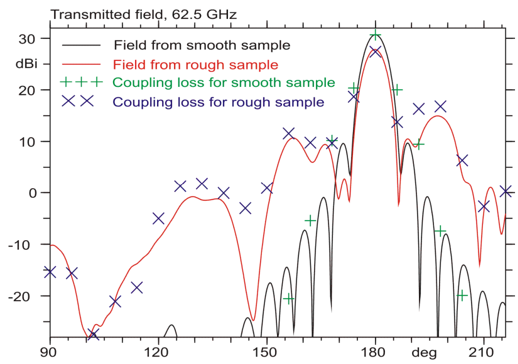

Fig. 11. Coupling values from dielectric smooth and rough sample for varying periscope rotations in transmission, compared with simple transmitted far-field of the sample.

As for the conducting rough sample, the coupling to VNA2 for a varying periscope rotation angle, with a dielectric smooth and rough sample, is compared to the nominal and distorted far-field in Fig. 11. It is seen that, a part from a scaling factor, the coupling values follow again extremely well the values of the far-field.

V. Detailed Analysis of the Periscope Walls

The scatterometer of Section III was drawn in detail by Thomas Keating, producing the CAD file shown in Fig. 12. A GRASP RF analysis of the influence of the scattering from the supporting structures and other unwanted ray paths was done, in order to check that the scatterometer was ready for the manufacturing phase, and if not, suggest the necessary modifications. The frequency of 62.5 GHz was chosen due to the larger beam waist, which increases the illumination of the structures near the mirrors. It was found that the field reflected by a smooth sample could, for periscope rotation angles between 80° and 100°, illuminate directly the sides of the periscope. The field from these currents is re-scattered in the periscope by the mirrors and the periscope side structures themselves. The received field on the TRM mirror must be computed by a full wave MoM calculation on the entire periscope sides and mirrors.

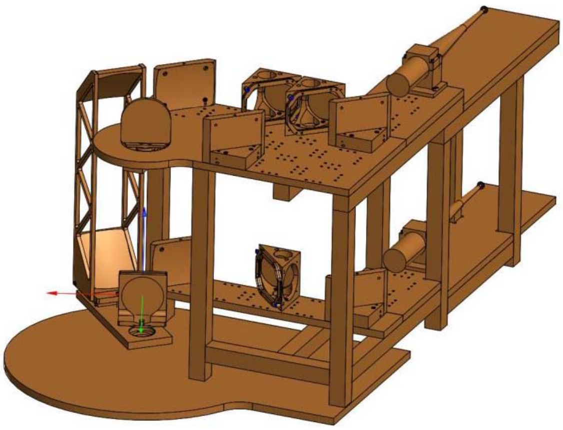

Fig. 12. CAD file of the detailed scatterometer imported in GRASP.

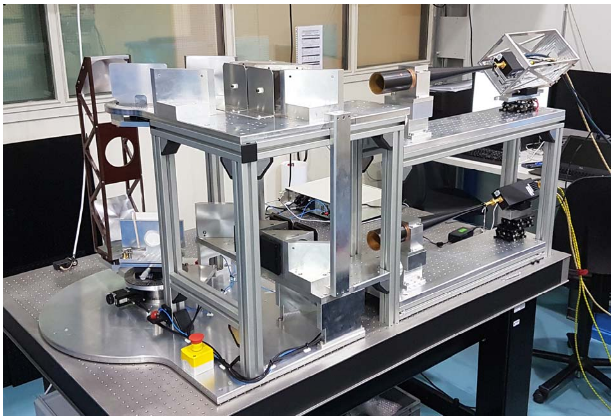

Fig. 13. Instrument manufactured and installed at ESA: the details of Fig. 2 and Fig. 12 are visible.

This gave rise in the worst case to a shift of the beam on VNA2 of 20 mm and a change in the peak value. It was thus decided to manufacture the sides of the periscope in dielectric material, Tufnol, to reduce reflections. A picture of the manufactured instrument is seen in Fig. 13.

VI. Conclusions

The previously reported design of a scatterometer for use in the 50-750 GHz range has been modelled using GRASP, to accurately compute the beam's quality and cross-polar performance over the full frequency band and a wide range of incidence and scattering angles. The RF performance of the scatterometer is calculated in GRASP using Physical Optics on all mirrors and the sample. For samples with roughness correlation lengths smaller than a wavelength, the Method of Moments add-on to GRASP is used on the sample. These methods give the exact RF scattering from the mirrors, where especially the offset ellipsoids generate higher order Gaussian modes. The power received by the VNA horn is extracted using the Coupling add-on to GRASP. The GRASP analysis showed that the initial design, designed with ray optics, suffered from poor cross-polar performances and beam quality.

A number of optical modifications were thus made an verified by GRASP, in order to arrive at a final design that could be manufactured and tested.

The GRASP software was used in the study to greatly improve the system performances in the design phase and, for the first time, accurately predict the scattering of rough samples in reflection and transmission over the 50 -750 GHz region of the spectrum for different incident angles. The scatterometer has been manufactured and is currently being tested.

References

[1] W. B. Weir, "Automatic measurement of complex dielectric constant and permeability at microwave frequencies," in Proc. of the IEEE 62, 1974, pp. 33-36.

[2] A. Krywonos, J. E. Harvey, and N. Choi, "Linear systems formulation of scattering theory for rough surfaces with arbitrary incident and scattering angles," Journal of the Optical Society of America A, vol. 28, pp. 1121-1138, 2011 2011.

[3] S. Z. Lo, D. Novotny, E. N. Grossman, and E. J. Heilweil, "Pulsed terahertz bi-directional reflection distribution function (BRDF) measurements of materials and obscurants," in Proc. SPIE 8022, 2011, pp. 80220G-8.

[4] R. Appleby et al., "A scatterometer for operation from 50 to 750 GHz", in Proc. of 38th ESA Antenna Workshop, ESTEC, Noordwijk, The Netherlands, 3-6 October, 2017.

[5] R. Appleby, E. Saenz, R. Wylde, and S. Froud, "Scattering in the THz region, measurement prediction and extrapolation," in Proc. European Conference on Antennas and Propagation (EuCAP 2014), 2014, pp. 2475-2477.